Geotechnical Parameters from Seismic Measurements: Two Field Examples from Egypt and Saudi Arabia

Mohamed H. Khalil[1] and Sherif M. Hanafy[1,2]
[1]Geophysics Dept., Faculty of Science, Cairo University, Cairo University Road, Giza, Egypt
Email: moh.hasan.khalil@gmail.com
[2]King Abdullah University of Science and Technology (KAUST), Thuwal, 23955-Jeddah, KSA
Email: sheriff.geo@gmail.com

ABSTRACT

Geotechnical parameters were used to determine subsurface rock quality for construction purposes. We summarize the mathematical relationships used to calculate the geotechnical parameters from P- and S-wave velocities and density values. These relationships are applied to two field examples; the first is a regional seismic study in Egypt and the second is a 2-D seismic profile recorded in Saudi Arabia. Results from both field examples are used to determine the subsurface rock quality and locate zones that should be avoided during construction. We suggest combining all geotechnical parameters into one map using a normalized-weighted relation, which helps to locate the zones with high versus low rock quality for engineering purposes.

Introduction

An essential step for robust new development is to understand the subsurface rock quality and structure. These two important aspects of the subsurface are sometimes difficult to efficiently quantify. This is because finding the geotechnical parameters of subsurface soil and rock usually requires direct measurements. For example, the cone penetrometer (CPT), which measures soil resistance to penetration and undrained shear strength, could lead to soil failure because it is an invasive experiment. This approach is direct and provides high resolution; however, it is expensive and has limited spatial significance.

Geophysical methods, such as the seismic method, offer a cheaper alternative with wider horizontal distribution, but with less resolution. Seismic methods have played an important role in the past few decades in solving engineering problems. They have been used to determine the subsurface rock sequences and locate structural features such as faults (Buddensiek *et al.*, 2008; Hanafy, 2012). Whenever shear-waves (S-waves) are measured, information about subsurface elastic properties can also be determined (Abd El-Rahman, 1989, 1991; Khalil and Hanafy, 2008). Although the seismic method is considered an indirect technique, it is inexpensive and provides the thickness and depth of subsurface layers. Table 1 provides a general comparison between the geotechnical and seismic approaches (Sobeira *et al.*, 2010).

Seismic methods have been used to solve engineering problems and to find geotechnical parameters for subsurface rock. One of the main applications in the early 1970's was directed at nuclear power plant siting. The Code of Federal Regulations of the United States Government (1974), known as the Weilas guidelines, published by the International Atomic Energy Agency (1972), are very specific regarding required investigations for potential plant sites. In response to these requirements, geophysical investigations were used to determine subsurface properties (layers, fluid saturation, and elastic moduli), structural complications (faults, voids or karst features), and the presence of underground water. In most instances, such determinations were required for only the first 100–200 m of the subsurface (Dobecki and Romig, 1985). Other applications included dam site investigations (Henriet *et al.*, 1983; Dutta, 1984; Kim *et al.*, 2010), groundwater resource exploration (Frohlich, 1974; van Overmeeren, 1975, 1980, 1981; Vandenberghe, 1976; Worthington, 1976, 1977; Carmichael and Henry, 1977), industrial plant foundation design (Dinis da Gama and Bernardo, 2002), fracture density and uniformity (*e.g.*, Bless and Ahrens, 1977; Sjogren *et al.*, 1979; Hamdi and Smith, 1981), dynamic processes monitoring, which includes groundwater, petroleum, mining, and geothermal provinces either by repeat, active survey methods or by continuous, passive survey monitoring (Dusseault and Nyland, 1982; Bartel, 1982; Holzhausen *et al.*, 1985; Arai and Tokimatsu, 2004; Goertz *et al.*, 2012), clay mapping (Bazin and Pfaffhuber, 2013; Adamczyk *et al.*, 2013; Shan *et al.*, 2014), void detection (Hanafy, 2010; Nolan *et al.*, 2011), and certification (safety) of existing structures such as dams (Bogoslovsky and Ogilvy, 1973a; Davenport and Hadley, 1984; Kim *et al.*, 2010), mines (Fajk, 1983; Hanafy *et al.*, 2009; Hanafy and Schuster, 2011), and concrete shafts (Hearne *et al.*, 1979).

 DOI: 10.2113/JEEG21.1.13

Table 1. Comparison between geotechnical and geophysical approaches to characterize the subsurface soils/rocks; after Sobreira *et al.* (2010).

	Geotechnical	Seismic
Scope (spatial significance)	Provides local information	Provides areal information
Resolution	High (centimeter scale)	Medium to low, but better toward surface (meter scale)
Strain regimes involved	High (rock failure)	Low (elastic domain)
Acquisition cost	Expensive	Very low

In this work, we are using the seismic refraction method (both P- and S-waves) with the measured density values to calculate the geotechnical parameters at two field sites. The first is located in Egypt, where ten P- and S-wave profiles were recorded and processed using the reciprocal method. The second field example is in Saudi Arabia, where one P-wave and one S-wave profile were collected and processed using first arrival traveltime tomography. In both field examples, the density values were found from rock samples extracted from boreholes. A total of seven different geotechnical parameters were calculated to study the quality of the subsurface rocks, and then these geotechnical parameter values were used to generate one contour map that summarizes all geotechnical results at the test sites.

Geotechnical Parameters

Geotechnical geophysics is defined by Sheriff (2002) as "The use of shallow geophysical methods of investigation in civil and construction engineering for road and building construction and evaluation, dam safety, and solution of related problems." In this definition, the geotechnical parameters are calculated using shallow geophysical methods to give a better understanding of the engineering condition of the subsurface rocks in the study area. In this work we used both P- and S-wave velocities, as well as density values, to find seven different geotechnical parameters, which allows classifying the area of study into different zones depending on the quality of the subsurface soils and rocks. These parameters are concentration and material indices, density gradient, stress ratio, N-value, bearing capacity, and reaction modulus. The following sections list the equation(s) used to calculate each of these geotechnical parameters.

Concentration Index (C_i)

Concentration index is an engineering parameter that is material dependent and indicates the degree of material concentration or competence for foundation and other civil engineering purposes. The main factors that control the concentration index are the elastic moduli of the materials and the depth-pressure distribution. Bowles (1982) formulated the concentration index in terms of Poisson's ratio (σ) as:

$$C_i = \frac{1+\sigma}{\sigma}, \tag{1}$$

where σ is Poisson's ratio and can be found as shown in Table 2. Abd El-Rahman (1991) defines C_i in terms of P- and S-wave velocities V_P and V_S as:

$$C_i = \left[3 - 4\left(\frac{V_S^2}{V_P^2}\right)\right] \Big/ \left[1 - 2\left(\frac{V_S^2}{V_P^2}\right)\right]. \tag{2}$$

Ranges of the concentration index are shown in Table 3.

Table 2. List of equations used to calculate elastic modulii. V_P and V_S are the P- and S-wave velocities, respectively.

Elastic modulus	Equation used	Reference
Poisson's Ratio	$\sigma = \frac{1}{2}\left[1 - \frac{1}{\left(V_P/V_S\right)^2 - 1}\right]$	Adams (1951), Salem (1990)
Young's Modulus	$E = \rho\frac{3V_P^2 - 4V_S^2}{(V_P/V_S)^2 - 1}$	Adams (1951)
Lame's Constants	$\lambda = \frac{\sigma E}{(1+\sigma)(1-2\sigma)}$	King (1966), Toksoz *et al.* (1976)
Shear Modulus	$\mu = \frac{E}{2(1+\sigma)}$	King (1966), Toksoz *et al.* (1976)
Bulk Modulus	$\kappa = \frac{3\lambda+2\mu}{3}$	Telford *et al.* (1976)

Material Index (M_i)

The material index defines the material quality for foundation purposes. It is an indicator of the degree of competence of a material and is based on the elastic moduli (Abd El-Rahman, 1989). It is influenced by the material composition, degree of consolidation, fracturing, jointing, and presence or absence of fluid in pore spaces, thus, affecting the wave velocity. The material index is given by:

$$M_i = 1 - 4\sigma = \frac{\mu - \lambda}{\mu + \lambda}, \tag{3}$$

where μ and λ represent the rigidity and Lame's constant, respectively. The values of μ and λ can be found using the equations shown in Table 2.

Density Gradient (D_i)

The density gradient, defined by Adams (1951), can be found either as a function of density (ρ) and bulk modulus (κ) or in terms of the compressional wave velocity (V_P) and Poisson's ratio (σ) (Adel El-Rahman, 1991):

$$D_i = \frac{3}{V_P^2} - \frac{1-\sigma}{1+\sigma} = \frac{\rho}{\kappa}. \tag{4}$$

The bulk modulus can be found from equations listed in Table 2. Higher values of the density gradient can be obtained in soil when slight changes in pressure decrease the porosity and increase the density. On the other hand, smaller values of density gradient can be expected in an indurated rock because of the lower porosity, higher confining pressure and pore fluids, which act against the applied load.

Stress Ratio (S_i)

During excess pressure caused by a stress change, a consolidation settlement occurs. By the end of the consolidation process, the excess pressure is nearly zero and the stress change will have gone from a total stress to an effective stress state. In this stress state, the soil state is defined as being an equilibrium steady-state condition of zero lateral and vertical strains (Bowles, 1982). Bowles (1982) gives the relation between the stress ratio and Poisson's ratio as:

$$S_i = \frac{\sigma}{1-\sigma}. \tag{5}$$

N-value (N)

The standard penetration test or N-value is applicable only for soils; it is not valid for rocks. It is defined according to Imai *et al.* (1976) and Stumpel *et al.* (1984) as the soil resistance to penetration by normalized cylindrically pointed bars under a standard load. The N-value is related to the shear wave velocity as:

$$N = \left(\frac{V_S}{76.55}\right)^{2.24719}, \tag{6}$$

where higher N-values indicate greater soil resistance to penetration, *i.e.*, higher cohesion soil.

Bearing Capacity (B_r)

The bearing capacity is defined as the maximum load required to produce soil shear failure. It can be evaluated according to Parry's formula (1977) by using the standard penetration test or N-value as:

$$B_r = \log(30N). \tag{7}$$

Reaction Modulus (R_m)

The reaction modulus, also known as modulus of subgrade reaction (Tribedi, 2013), gives the relationship between soil pressure and deflection (Moayed, 2012), and is measured as load intensity per unit of displacement (Tribedi, 2013):

$$R_m = \left(\frac{V_S}{80.5}\right)^{1/0.357}. \tag{8}$$

It is one of the most efficient parameters used for structural analysis of foundation members. The popular practical method for estimating the R_m is the plate load test (PLT), which determines the ratio of load to displacement of a circular plate with 15-cm to 75-cm diameter (Terzaghi, 1955). The reaction modulus is dependent on parameters such as soil type, size and shape of foundation, depth and stress level.

The ranges of the engineering parameters and the corresponding rock (soil in case of N-value, bearing capacity, and reaction modulus) quality are summarized in Table 3. This table is gathered from the results of our field examples listed in this work as well as the work of Birch (1966), Gassman (1973), Tatham (1982), Sheriff and Geldart (1986), and Abd El-Rahman (1989, 1991).

Field Examples

We applied the geotechnical parameters equations given in this work on two field examples. The first is a data set collected in Egypt, whereas the second is a data set collected in Saudi Arabia.

Field Example 1: General Seismic Study

Dakhla is one of the few oases located at the western desert of Egypt. It lies between latitude 25° 28′ to 25° 44′ North and longitude 28° 48′ to 29° 21′ East (Fig.1). The Dakhla Oasis spans an area of about 410

Table 3. The range of engineering parameters and the corresponding rock/soil type. Information in this table is gathered from our results in this work and Birch (1966), Gassman (1973), Tatham (1982), Sheriff and Geldart (1986), and Abd El-Rahman (1989, 1991).

		Weak		Fair		Good
		Very Soft	Soft	Fairly Compacted	Moderately Compacted	Compacted
Rock	Concentration Index (C_i)	3.5–4.0	4.0–4.5	4.5–5.0	5.0–5.5	5.5–6.0
	Material Index (M_i)	<–0.6	−0.6 – −0.2	−0.2–0.2	0.2–0.6	0.6–1.0
	Stress Ratio (S_i)	0.7–0.61	0.61–0.52	0.52–0.43	0.43–0.34	0.34–0.25
Soil	N-value (N)	0–250	250–500	500–750	750–1,000	1,000–1,200
	Bearing Capacity (B_r)	2–2.6	2.6–3.2	3.2–3.8	3.8–4.4	4.4–5.0
	Reaction Module (R_m)	0–1,200	1,200–2,400	2,400–3,600	3,600–4,800	4,800–6,000

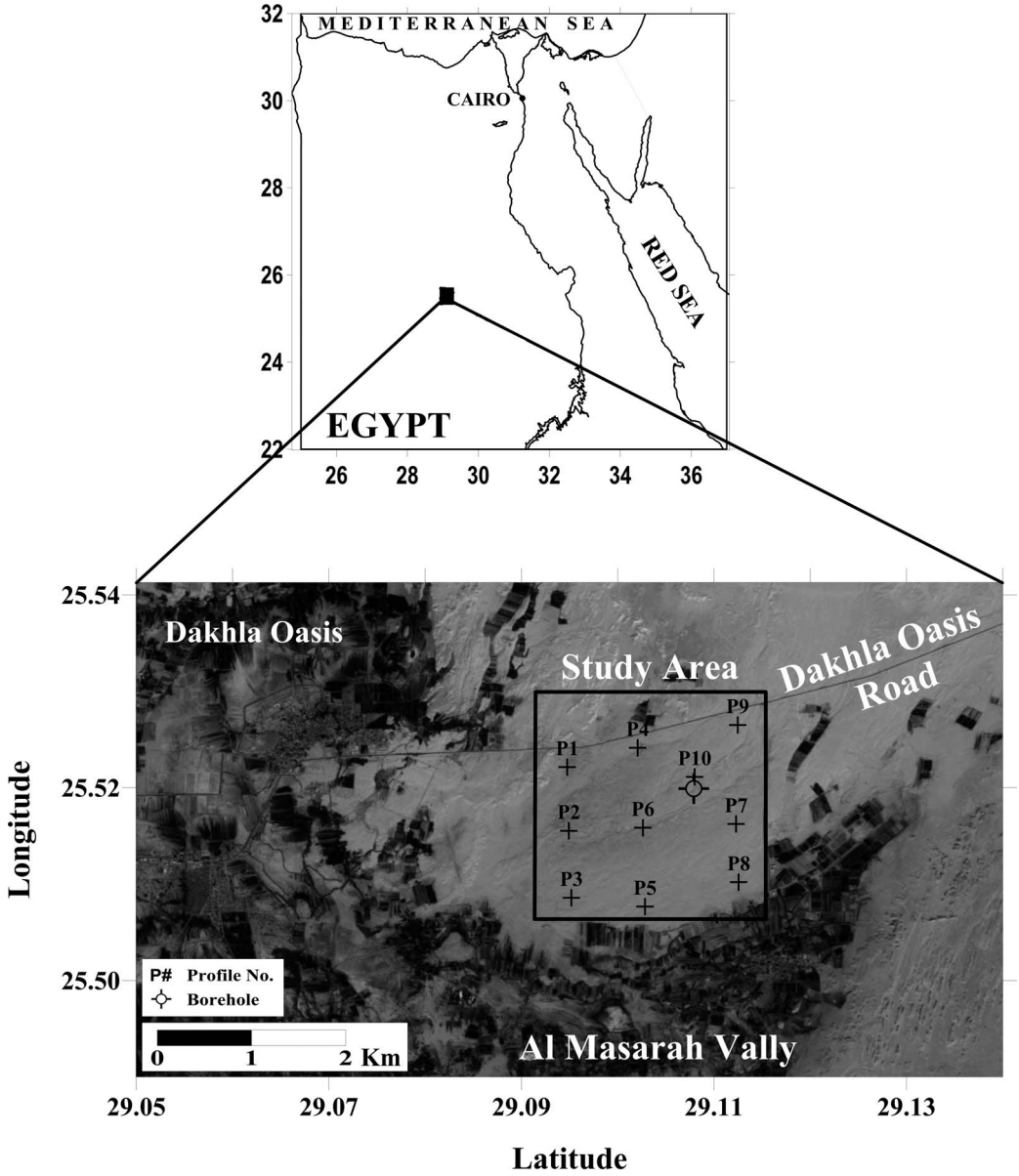

Figure 1. Locations of the seismic profiles at Dakhla Oasis, Western Desert, Egypt.

km^2 and is located approximately 120 kilometers west of Kharga Oasis. This oasis consists of 14 settlements and has a population of about 70,000 inhabitants; most of them are farmers. Dakhla is the farthest oasis from Cairo and is considered one of Egypt's most beautiful oases.

The Dakhla oasis occupies a structurally localized depression below a 300 to 400 m escarpment bordering the Libyan Plateau and the Western Desert of Egypt at 90–140 m above sea level. The scarp runs for 200 km east-southeast to west-northwest along the northern edge of the depression. The 300- to 400-m high scarp is composed of a top layer of white chalky limestone followed by a mid-section of "greenish and ash-grey leafy clays" and has a base of brown and black beds containing gypsum and scattered deposits of fossils. Between the scarp and the cultivated areas from Qasr Dakhla in the west to beyond Tineida in the east there is a dark-brown layer that is mainly composed of fish, fish teeth, bones, and vertebrate fossils and has a thickness of 2 to 3 m. This fossiliferous bed is associated with phosphate and used as fertilizer. Other minerals found in the area include ocher, cobalt, nickel, salt, and barites. There are also black and red clays, the latter containing iron oxide (Brookes, 1989, 1993). Most of the mudbrick buildings in the oasis are tinged with the red of iron oxide.

The northern escarpment is the major cliff in Dakhla. The eastern part of the oasis is open to the Kharga Oasis, the west is blocked by the massive dunes of the great Sand Sea, and the south drops over a minor escarpment and then runs free for hundreds of kilometers past the Gilf Kebir and into Sudan.

The Nubian Sandstone Aquifer System, which is the main aquifer in this area, is a closed, non-renewable transboundary groundwater system of massive thickness and high water storage capacity. It has been undergoing arid to hyper-arid conditions and has had no significant recharge for about 5,000 years. It has a wide extent over Egypt, southeastern Libya, northeastern Chad, and northwestern Sudan and lies between latitudes 14° and 30° N and longitudes 19° and 34° E. The aquifer consists mainly of four structural basins, the major among them are the Kufra Basin and the Dakhla Basin. The aquifer comprises an area of about 2.35×10^6 km² and has a maximum thickness of 4,500 m. The ground surface of the aquifer reveals a general slope from SSE to NNW and ranges roughly from about 3,000 m to −134 m above mean sea level (amsl). The hydraulic head ranges from 570 m (amsl) west of the Darfur area in Sudan to −78 m in the north of the system, in the Qattara Depression in Egypt. The modeled geometric volume is about 3.5×10^6 km³ and the calculated groundwater volume is about 212×10^3 km³. The exploitation of the aquifer resources is increasing rapidly, forming large cones of depression around the groundwater extracting fields. These hydrogeological data are based on Said (1962, 1990).

The existence of ground water in this area makes it a good candidate for future engineering development. However, geophysical studies in the western desert of Egypt are rare, thus information about the subsurface rock quality is missing. We chose this area to conduct a regional geophysical study and calculate the engineering parameters, which is a first step for a more detailed study in the future.

In this field example, we collected ten seismic profiles at Dakhla Oasis, Western Desert, Egypt (Fig. 1). Each profile contains three shot locations at offsets of X = 0, 27.5, and 55 m, where 12 receivers with a receiver interval of 5 m are used, except for the first and last receivers where the shot-receiver offset was 1 m. At each receiver location we used P- and S-wave receivers to collect both the compressional (P) and the shear (S) signals. P- and S-waves were generated using an 8-kg sledgehammer hitting a small metallic plate. During the P-wave data acquisition, the plate was placed horizontally. For the S-wave collection, the plate was placed at a 45 degree angle and hit on both sides. The two S-wave traces were recorded at each receiver and one subtracted from the other to eliminate the P-wave and enhance the S-wave.

To process the recorded P- and S-wave data sets, we followed the following four steps:

1. The first arrival traveltimes of the recorded data (P- and S-waves) are picked.
2. The reciprocal method (Hawkins, 1961) is used to interpret the picked traveltimes and generate the initial velocity–depth model of each P- and S-profile.
3. The result is verified using the finite difference method (Vidale, 1988, 1990; Qin *et al.*, 1992) as described by Hanafy (2005). Here, the velocity–depth model generated from the reciprocal method is used as the input velocity model for the finite difference method and the first arrival traveltimes are synthetically calculated and compared to the observed times.
4. If the differences between the observed and calculated traveltimes are larger than a pre-defined RMS error value, then the velocity–depth model is manually modified and step 3 is repeated until the differences between the calculated and observed traveltimes are within an accepted error margin, $\pm$ 5% in our case.

Following these four steps will produce the V_P and V_S values at each profile location. In this study, we considered only the P- and S-wave velocities of the bedrock (Fig. 2 and Table 4). The densities were measured in the laboratory from rock samples taken from a borehole near profile #10 (Fig. 2). Depth to the top of the bed rock ranges between 6 and 9 m from ground surface

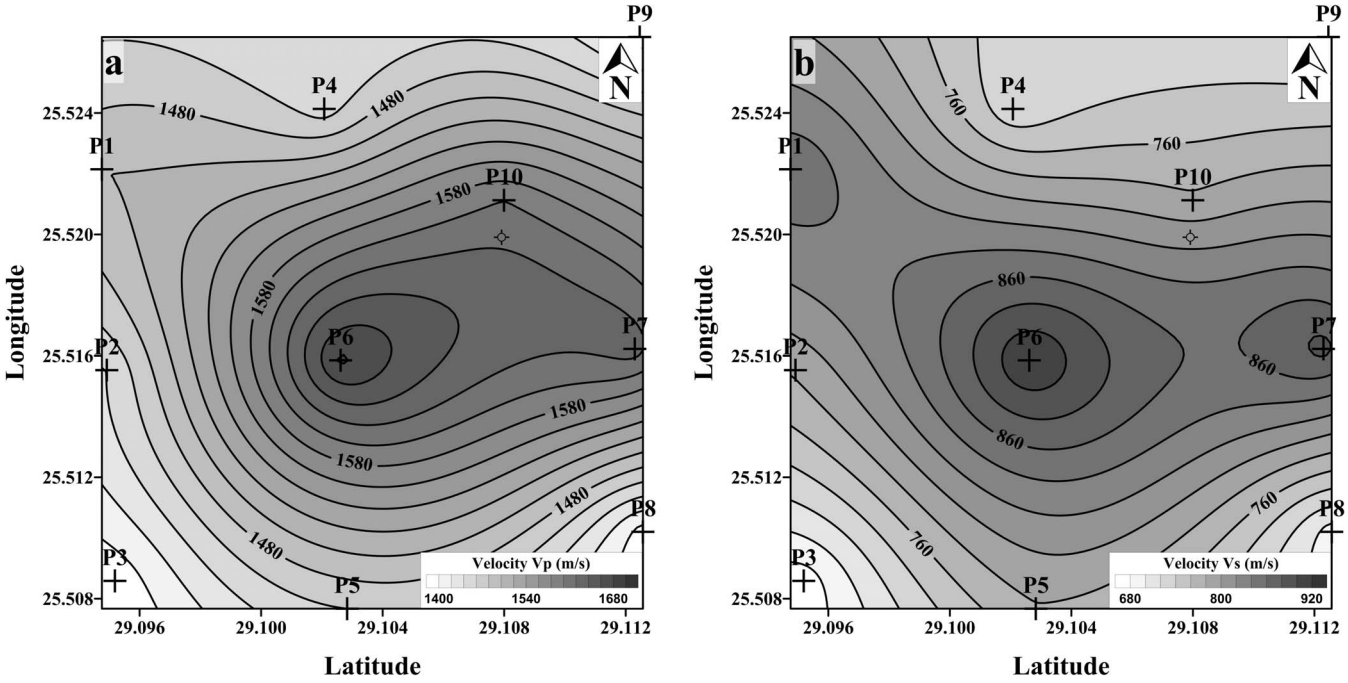

Figure 2. P-wave velocity (a), and S-wave velocity (b) contour maps of Dakhla Qasis study area.

(Table 4). The P-, S-wave velocities and density values are then used to calculate the elastic moduli (Table 2), and hence the geotechnical parameters listed in Eqs. (1) to (8). Two different subsurface layers can be identified in the seismic profiles: 1) a surface layer consisting of dry sand-silt deposits with P-wave velocity ranging between 380 m/s and 450 m/s, and S-wave velocity ranging between 140 m/s and 210 m/s; and 2) a highly-fractured sandstone layer partially saturated with water. We consider this layer as the bedrock; the depth to the top of this layer and the P- and S-wave velocities are shown in Table 4.

The geotechnical parameter values are shown as contour maps in Figs. 3 and 4. The contour maps of the geotechnical parameters show that the northwestern corner of the study area is characterized by subsurface rocks of lower quality than the rest of the study area. The values of the minimum and maximum geotechnical parameters in this field example lie within the moderate to high rock quality designation (Table 3).

In this work, we show the results of seven different geotechnical parameters (Figs. 3 and 4). It is understood that the importance of each of these geotechnical parameters is not the same; some of them are more important or more representative of the sediments' quality than others. Hence, we introduce a weighting factor (W) that reflects the importance of each of these geotechnical parameters. To summarize the geotechnical parameter results into one contour map (called a contribution map), we use Eq. (9) as described in the following steps:

1. The values of each geotechnical parameter are normalized to its maximum value.
2. Each geotechnical parameter is multiplied by its weighting factor.

Table 4. V_P and V_S values used to calculate the geotechnical parameters at the first field examples. Both V_P and V_S are calculated using field seismic data, then interpreted using the reciprocal method and adjusted by the finite difference method. The bottom row shows the depth to the top of the bedrock in meters.

Profile	1	2	3	4	5	6	7	8	9	10
V_P (m/s)	1,500	1,440	1,385	1,450	1,460	1,684	1,630	1,390	1,410	1,600
V_S (m/s)	857	783	668	725	778	921	887	690	720	784
Z (m)	7.2	8.8	8.0	7.2	6.8	8.2	6.5	6.3	7.3	7.5

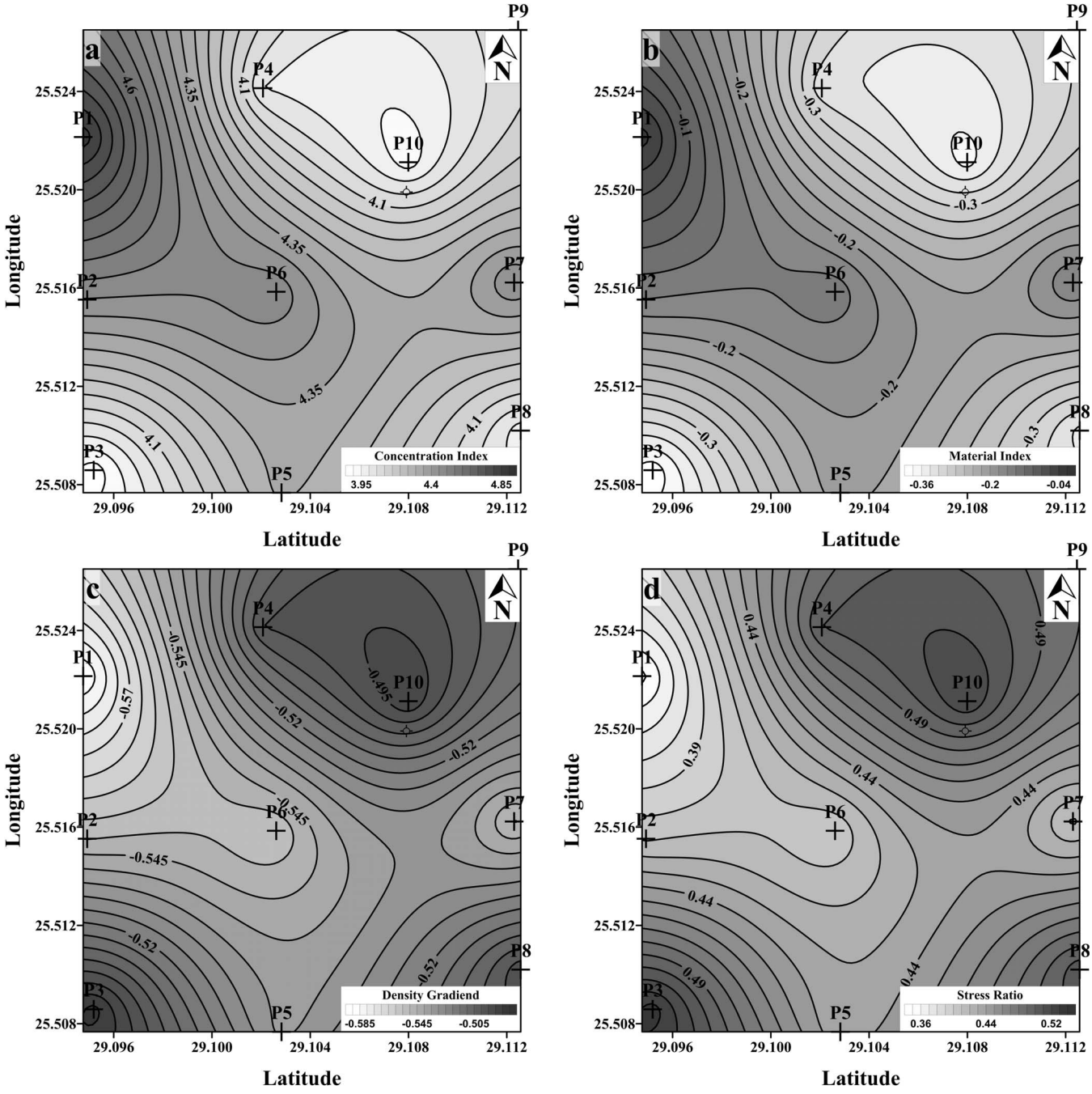

Figure 3. The geotechnical parameters for field example #1: a) concentration index, b) material index, c) density gradient, and d) stress ratio.

3. The weighted-normalized geotechnical parameters at each grid point are stacked to get the contribution map values.
4. The contribution map values are then normalized and contoured (Fig. 5):

$$C_m(x,y) = \frac{1}{m}\sum_{i=1}^{m} W_i \frac{P_i(x,y)}{\max|P_i|}, \tag{9}$$

where $C_m(x, y)$ is the contribution value of all geotechnical parameters at point (x, y), P_i is a variable that refers to the corresponding geotechnical parameter, W_i is a weight depending on the geotechnical parameters, and m is the total number of geotechnical parameters. For example, in our case we have seven different geotechnical parameters (m = 7), and assume that the concentration index (C_i) is parameter # 1, …., reaction modulus is parameter #7, then $P_1 = C_i$, …, $P_7 = R_m$.

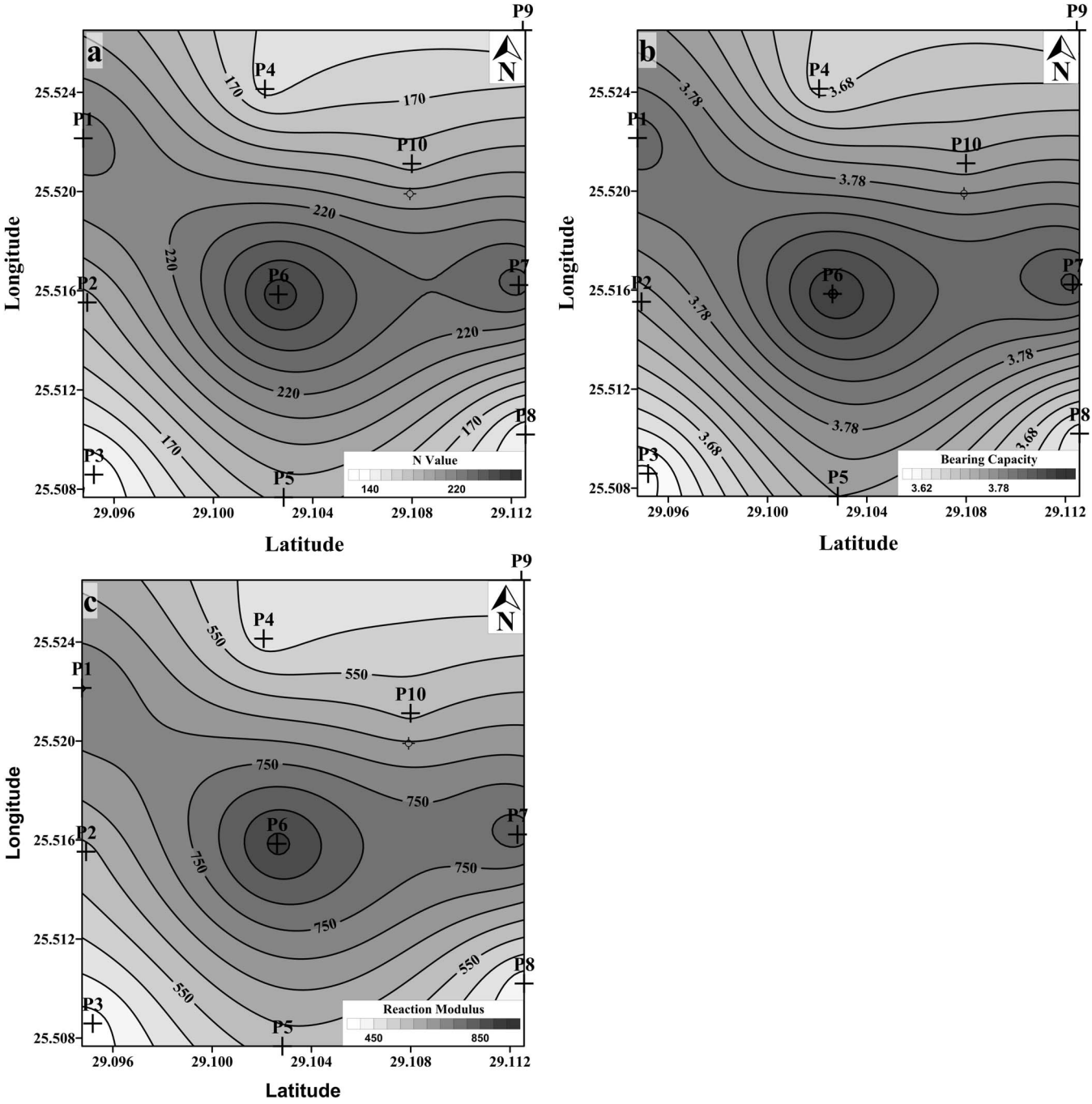

Figure 4. The geotechnical parameters for field example #1: a) N-value, b) bearing capacity, and c) reaction modulus.

An important point here is how to determine the weighting factor for each geotechnical parameter. This depends on the target of the study and what we want to focus on as a final result. We suggest using three different values for the weighting factor, 0.5, 1, or 2. A value of 0.5 is assigned to geotechnical parameters that are not essential in our study, 2 is assigned to the important geotechnical parameters, while 1 is assigned to all other geotechnical parameters. This point needs further study and more examples.

Figure 5 shows the contribution contour map (C_m) that summarizes all geotechnical parameters of the first field example. The values of C_m reflect the quality of the subsurface sediments. In this field example all C_m values are greater than 0.5, which means a moderate to good sediment quality. However, Fig. 5 shows higher

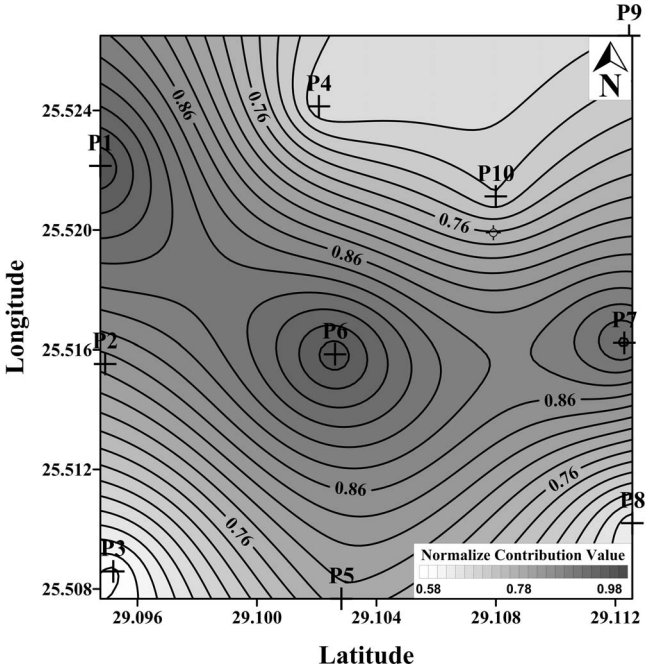

Figure 5. A contour map showing the contribution values calculated using Eq. (9). The northwestern and central parts of the study area show a better rock quality.

C_m values at the northwestern corner and central parts of the study area, which indicates a better sediment quality in these areas. A more detailed study could be required at construction sites of more important facilities, such as water and power stations.

Field Example 2: 2-D Profile

The first field example is considered a general study of the area of interest, as it gives a general overview of the subsurface rock quality. For a more detailed study, we present field example #2. In this example, we present the results of a 2-D profile collected in western Saudi Arabia (Fig. 6). Here, we used 120 shot gathers at 5-m shot intervals and 240 receivers/shot gathers at 2.5-m receiver interval. We collected both P- and S-wave data sets using P- and S-wave receivers and P- and S-wave data acquisition as described in field example #1 (Fig. 7). This data set was collected to find the exact location of the Qademah Fault (Fig. 6).

The two data sets are inverted using first arrival traveltime tomography to generate the V_P and V_S traveltime tomograms (Fig. 8). The P-wave velocity (Fig. 8(a)) shows a range of 500 to 3,000 m/s, while the S-wave velocity (Fig. 8(b)) shows a range of 150 to 2,000 m/s. Three different subsurface layers can be identified in this example: 1) the surface layer, which consists of loose sand, silt, and gravel sediments, the thickness of this layer ranges between 2 to 6 m; 2) the second layer is characterized by fractured limestone partially saturated with saline water and has a thickness of 20 to 30 m; and 3) the third layer, which is the bed rock, is characterized by a compact limestone at a depth of 50–60 m from the ground surface. The fault location is not very clear on the traveltime tomograms; however, the low velocity anomaly located between X = 100 m and X = 200 m on the V_P section, and X = 100 m and X = 220 m on the V_S section could be an indication of the colluvial wedge associated with the Qademah fault (Hanafy, 2012).

We extracted rock samples from a water well near the area of study to determine the density values. The V_P, V_S, and density values were then used to calculate the geotechnical parameters (Figs. 9 and 10) using the equations listed in Table 2 and Eqs. (1) to (8). The location of the colluvial wedge associated with the Qademah fault is evident on the concentration index and material index plots (Figs 9(a)–(b)) as low values, and on both density gradient and stress ratio plots (Figs. 9(c)–(d)) as high values; it is located between X = 150 and X = 210 m. This shows that the geotechnical parameters have the power to show local anomalies with higher resolution than using only velocity models. On the other hand, the pseudo N-value does not show the fault location; however, it shows a gradual increase with depth. Here, we used the word "pseudo" since the N-value is used to characterize soils and not consolidated rocks.

The contribution map of the second field example is shown in Fig. 11. In this example, the contribution values range between 0 and 1 for very low to very high rock quality, respectively. From Fig. 11 we can locate zones with low rock quality, which should be avoided during construction. The low rock quality zones are where the contribution values are less than 0.2; between X = 0 and X = 150 m and depth Z = 0 and Z = 30 m, and the fault zone (X = 150 to X = 210 m) up to a depth of 60 to 70 m from the ground surface.

The low rock quality zones shown in Fig. 11 are associated with the Qademah fault. This example clearly shows the importance of the geotechnical parameters and the contribution map, where, looking at the contribution-value's map summarizes all geotechnical parameters result and guides us to the zones of high vs. low quality subsurface rock.

Discussion

The relationship between geophysical measurements (V_P, V_S and density) and geotechnical parameters has been studied in this work using two field examples. In the first field example we discussed how to find the geotechnical parameters for a regional study, where distances between profiles are great and the number of shots in each profile is limited. We processed each profile

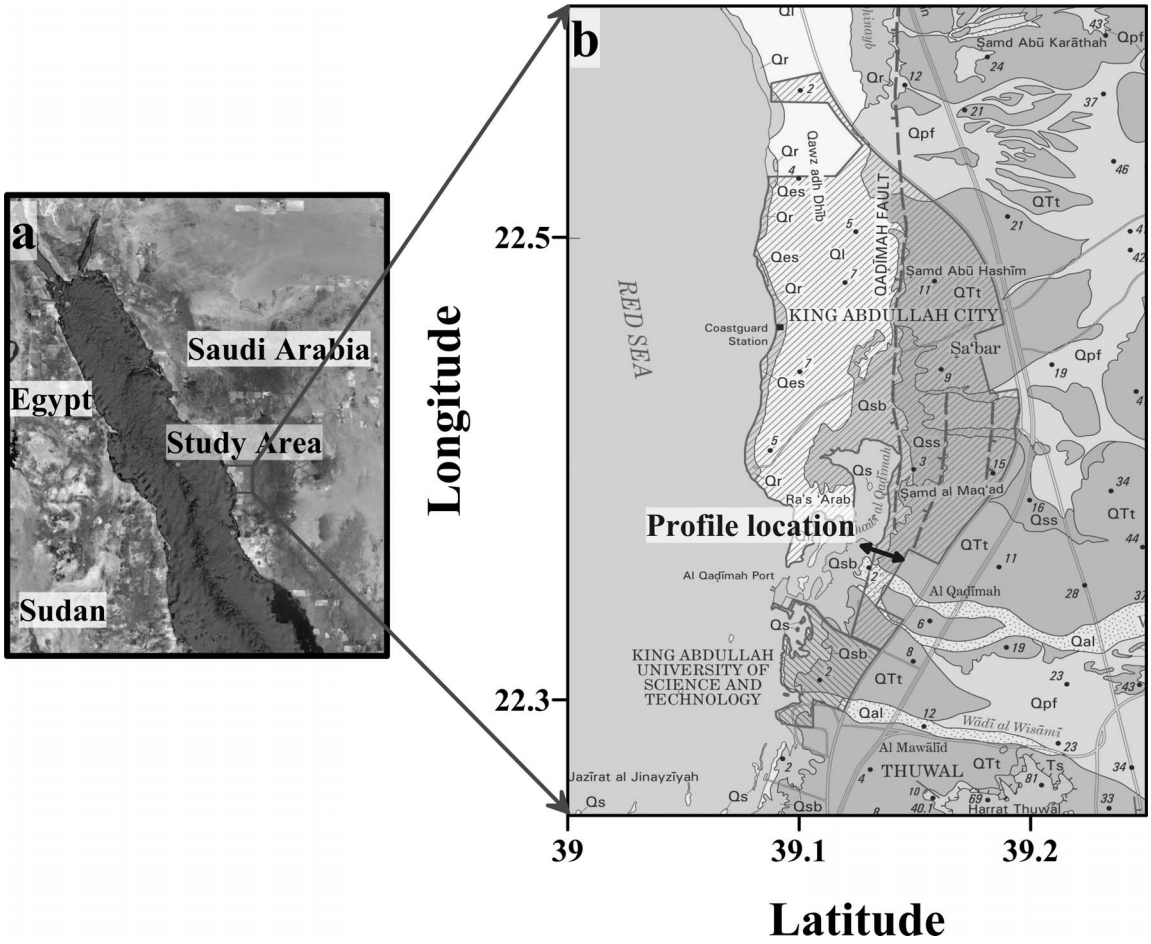

Figure 6. Study area located in the western region of Saudi Arabia. b) Map showing the locations of the seismic profiles (black double-arrow line) at field example #2, Qademah area, Saudi Arabia.

and generated the velocity–depth section for both V_P and V_S, then one V_P and one V_S value was selected to represent each layer of interest. For plotting purposes, the selected velocity values were located at the center of the profiles. All geotechnical parameters could then be calculated, providing the density value, and, hence, contour maps were generated to show the lateral distribution of each geotechnical parameter. We suggested a further step, where all geotechnical parameters are blended together to generate one representative contour map, called the contribution map. The contribution values are calculated using weighted-normalized geotechnical values. The weight used here primarily depends on the importance of each geotechnical parameter. In this study, we used equal weights for simplicity.

In the second field example we discussed a more detailed field test, where V_P and V_S tomograms are generated using first arrival travel times. Here, the variations in the geotechnical parameters can be found in both lateral and vertical directions, which give more details about the quality of the subsurface rocks.

An important issue is selecting the weight value(s) for each geotechnical parameter. This selection could depend on the purpose of the study, *i.e.*, the geotechnical parameter that is more important to the purpose of the study will have a higher weight value. The weight value could also be a constant number that is multiplied by the corresponding geotechnical parameters after normalization or can be a vector that is multiplied by the geotechnical parameter vector.

The calculations of the geotechnical parameters mainly depend on the values of V_P and V_S, assuming that the density is constant. The variations in the density values in the near-surface applications are, in general, limited and can be considered constant. Accepting this assumption, we can generate the contribution values for different V_P and V_S values (Fig. 12). This figure gives an indication of the quality of the subsurface rock

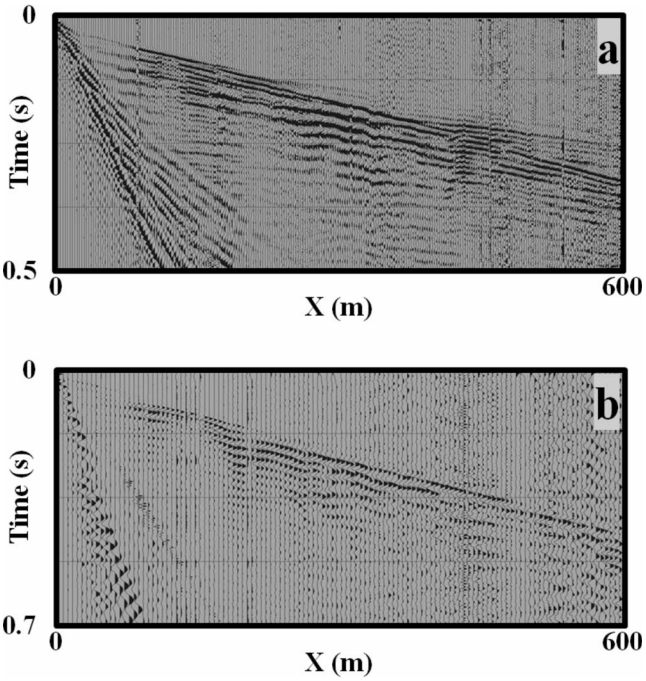

Figure 7. Two shot gather examples from field example #2, Qademah data: a) P-wave shot gather #1 and b) S-wave shot gather #1.

knowing only V_P and V_S values without the need to calculate all geotechnical parameters. Here, we found the contribution values for V_P ranges between 600 and 3,000 m/s, V_S ranges between 200 and 1,800 m/s, and the V_P / V_S ratio ranges between 1.4 and 3. As expected, the contribution value is greater for higher V_P and V_S values. Contribution value plots, such as Fig. 12, are an expedient method for determining the subsurface rock quality when only V_P and V_S data are available.

Conclusions

In this work, we summarized the elastic moduli and geotechnical parameter relationships as derived from V_P, V_S, and density values. In seismic field work, both V_P and V_S can be calculated using refraction data, while the density is found from rock samples.

To show the importance of these parameters we presented two field examples, the first is a regional seismic study at Dakhla Oasis, Western Desert, Egypt. In this example we collected ten P- and S-wave profiles, and found density values from a borehole near profile #10. The V_P and V_S were calculated using the reciprocal method, then V_P, V_S, and density values were used to find elastic moduli and produce geotechnical parameter

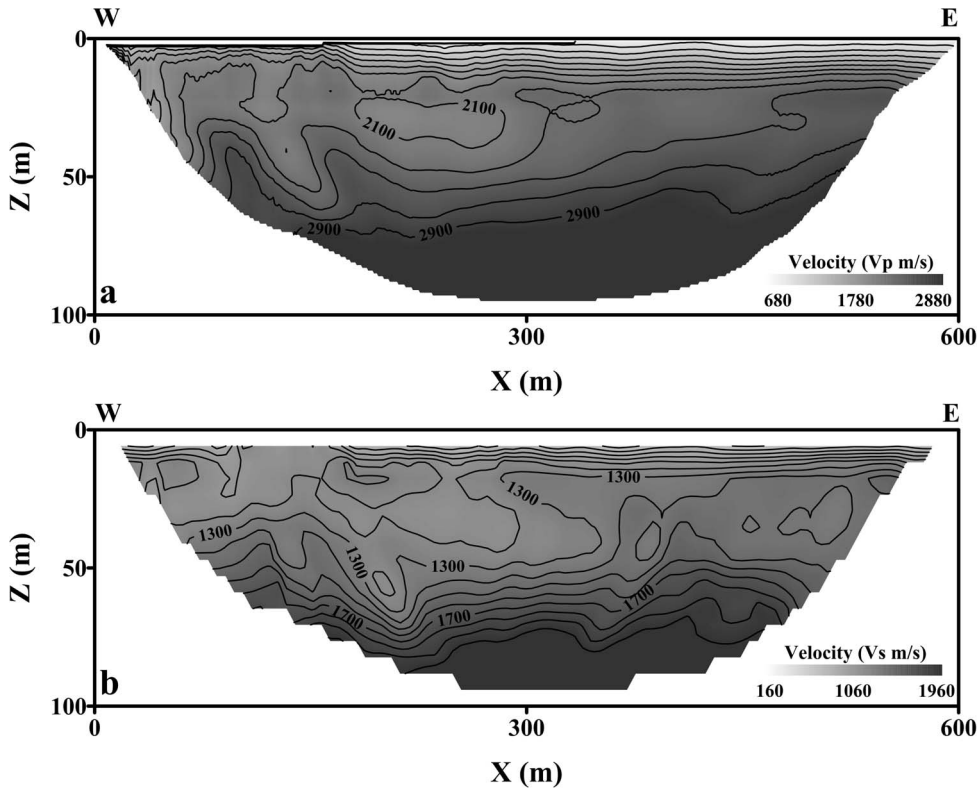

Figure 8. P-wave (a) and S-wave (b) velocity tomograms at field example #2, Qademah study area.

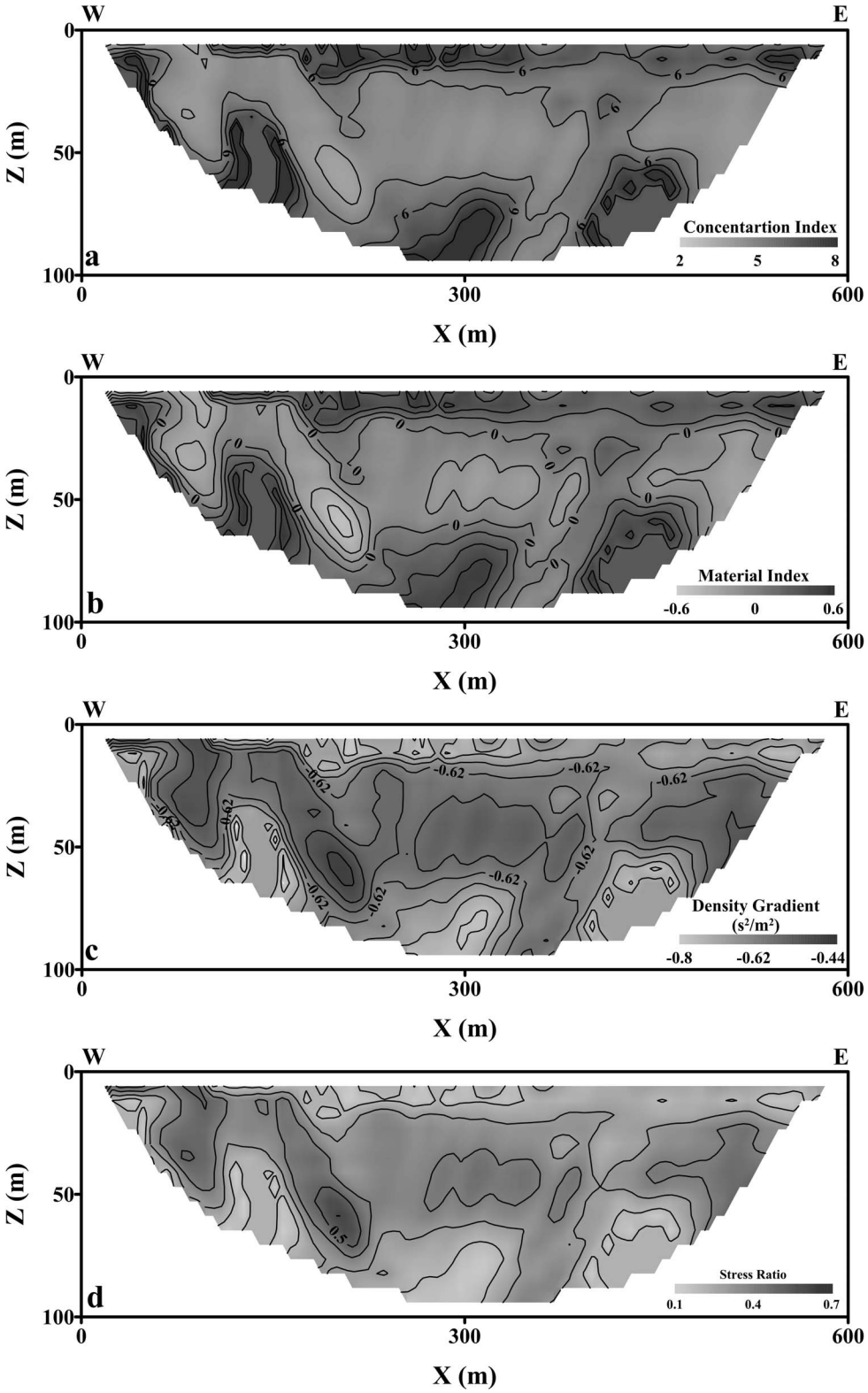

Figure 9. The geotechnical parameters for field example #2: a) concentration index, b) material index, c) density gradient, and d) stress ratio.

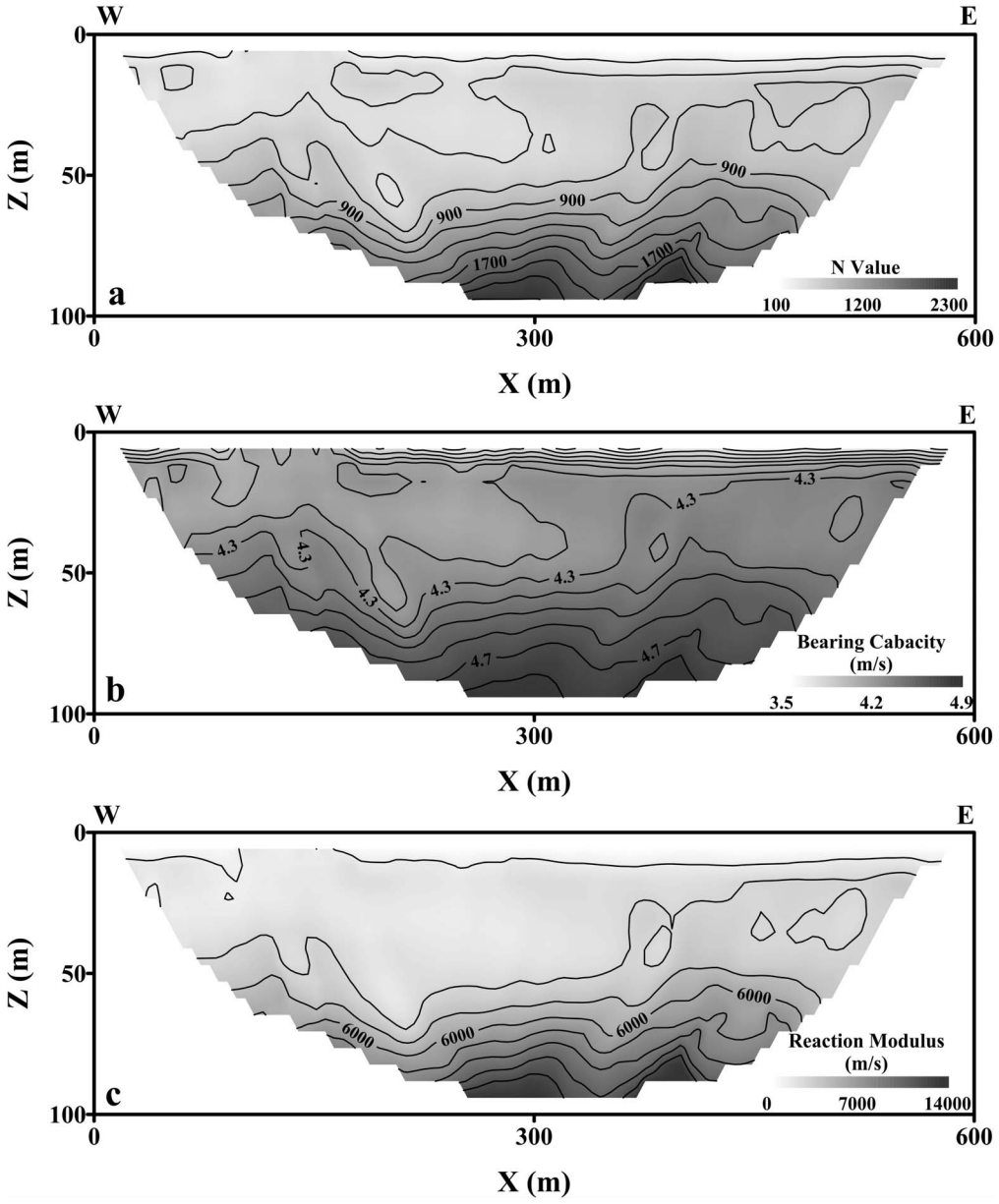

Figure 10. The geotechnical parameters for field example #2: a) pseudo N-value, b) bearing capacity, and c) reaction modulus.

contour maps. A contribution map was then generated, which summarized the geotechnical parameters in one map. The contribution map of field example #1 showed values greater than 0.5, which indicates good subsurface rock quality; no evidence of low rock quality can be seen in the contour map sets of this field example.

The second field example is considered to be a detailed subsurface study, where P- and S-wave data were collected along one 2-D profile 600 m in length. The first arrival traveltimes were picked, then inverted to find both the V_P and V_S tomograms. The density values were calculated from rock samples extracted from a water borehole near the area of study. The aim of this data set was to locate a normal fault called Qademah. The exact location of the Qademah fault on both the V_P and V_S tomograms was not clearly defined. However, the colluvial wedge associated with the Qademah fault is evident on the geotechnical parameters maps. The contribution map of the second field example exhibited a range of 0 (low rock quality) to 1 (high rock quality), and the location of the colluvial wedge associated with the fault is well defined in this map. Using the

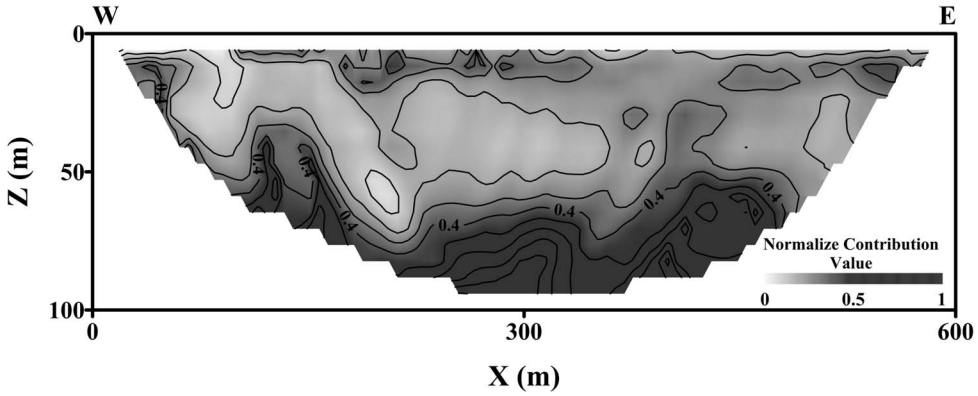

Figure 11. 2-D profile showing the contribution values calculated using Eq. (9). Areas with contribution value >0.4 show a better rock quality.

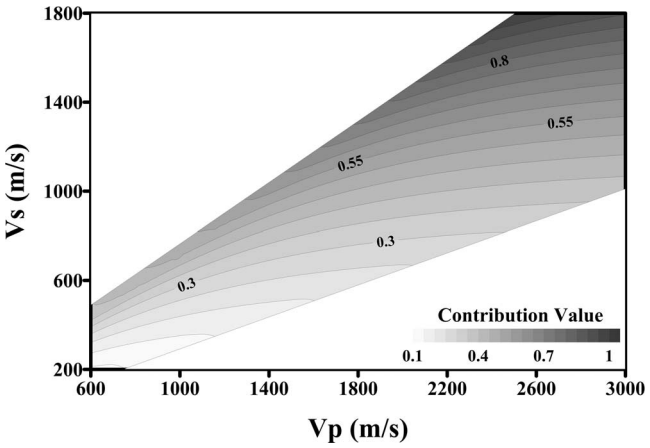

Figure 12. The contribution values for V_P between 600 and 3,000 m/s, V_S between 200 and 1,800 m/s, and V_P / V_S ratio between 1.4 and 3.0, assuming a constant density of 2.0 g/cm^3.

contribution map, we can easily determine the locations of low rock quality that should be avoided, or given special consideration, during any construction process.

Acknowledgements

We would like to thank Yunsong Huang and James Argyle for the valuable suggestions and manuscript revision they provided.

References

Abd El-Rahman, M., 1989, Evaluation of the kinetic elastic modulii of the surface materials and application to engineering geologic maps at Maba-Risabah area (Dhamar Province), Northern Yemen, Egypt: J. Geol., **33**(1-2) 229–250.

Abd El-Rahman, M., 1991, The potential of absorption coefficient and seismic quality factor in delineating less sound foundation materials in Jabal Shib Az Sahara area, Northwest of Sanaa, Yemen Arab Republic, Egypt, M. E.R.C.: Ain Shams University, Earth Science, **5**, 181–187.

Adamczyk, A., Malinowski, M., and Malehmir, A., 2013, Application of first arrival tomography to characterize a quick clay landslide site in Southwest Sweden: Acta Geophysica, **61**, 1057–1073, doi:10.2478/s11600-013-0136-y.

Adams, L.H., 1951, Elastic properties of materials of the earth's crust. Internal construction of the earth (edited by Gutenberg): Dover Publications, Inc., New York.

Arai, H., and Tokimatsu, K., 2004, S-wave velocity profiling by inversion of microtremor H/V spectrum: Bulletin of the Seismological Society of America, **94**, 53–63, doi:10.1785/0120030028.

Bartel L.C., 1982, Modeling and analysis of the CSAMT geophysical technique results to map oil recovery processes: 57th Ann. Tech. Conf., Soc. Petr. Eng., Am. Inst. Min. Metall. Petr. Eng., Paper SPE 11192.

Bazin, S., and Pfaffhuber, A.A., 2013, Mapping of quick clay by electrical resistivity tomography under structural constraint: Journal of Applied Geophysics, **98**, 280–287, doi:10.1016/j.jappgeo.2013.09.002.

Birch, F., 1966, Handbook of physical constants: Geol. Soc. Amer. Mem., **96**, 613 pp.

Bless, S.I, and Ahrens, T.J., 1977, Measurement of the longitudinal modulus of Pierre clay shale at varying strain rates: Geophysics, **42**, 34–40.

Bogoslovsky, V.A., and Ogilvy, A.A., 1973a, Deformations of natural electric fields near drainage structures: Geophys. Prosp., **21**, 716–723.

Bogoslovsky, V.A., and Ogilvy, A.A., 1973b, Electrometric observation of antifiltration cementation curtains: Geophys. Prosp., **21**, 296–314.

Bowles, J.E., 1982, Foundation analysis and design: McGraw-Hill International Book Company, London (2nd Ed.), 587 pp.

Brookes, I., 1989, Early Holocene basinal sediments of the Dakhleh Oasis Region, South Central Egypt: Quaternary Research, **32**, 139–152.

Brookes, I., 1993, Geomorphology and Quaternary geology of the Dakhla Oasis Region, Egypt: Quaternary Science Reviews, **12**(7) 529–552, doi:10.1016/0277-3791(93) 90068-W.

Buddensiek, M.L., Sheng, J., Crosby, T., Schuster, G.T., Bruhn, R.L., and He, R., 2007, Colluvial wedge imaging using traveltime and waveform tomography along the Wasatch fault near Mapleton, Utah: Geophys. J. Int., **172**, 686–697, doi:10.1111/j.1365-246X.2007. 03667.x.

Carmichael, R.S., and Henry, G. Jr., 1977, Gravity exploration for groundwater and bed rock topography in glaciated areas: Geophysics, **42**, 850–859.

Davenport, G.C., and Hadley, L.M., 1984, Outlet pipe logging, southside reservoir: Unpublished report to Southside Irrigation District, Loveland, Colorado.

Dinis da Gama, C., and Bernardo, P.M., 2002, Geological, geotechnical and microvibration studies in sensitive foundation sites: *in* Proc. 8th National Congress of Geotechnics, Lisbon, 1925–1935.

Dobecki,T.L., and Romig, P.R., 1985, Geotechnical and groundwater geophysics: Geophysics, **50**, 2621–2636.

Dusseault, M.H., and Nyland, E., 1982, Fireflood rnicroseismic monitoring-rock mechanics irnplications: *in* Issues in Rock Mechanics, 23rd U.S Symposium on Rock Mechanics (USRMS), 25–27 August, Berkeley, California.

Dutta, N.P., 1984, Seismic refraction method to study the foundation rock of a dam: Geophys. Prosp., **32**, 1103–1110.

Fajk, L.Z., 1983, Rock burst forecasting and genetic research in coal-mines by microgravity method: Geophys. Prosp., **31**, 748–766.

Frohlich, R.K., 1974, Combined geoelectric and drill-hole investigation for detecting fresh-water aquifers in northwestern Missouri: Geophysics, **39**, 340–352.

Gassman, F., 1973, Seismic prospection: Birkhaeuser Verlag, Stuttgart, 417 pp.

Goertz, A., Schechinger, B., Witten, B., Koerbe, M., and Krajewski, P., 2012, Extracting subsurface information from ambient seismic noise - A case study from Germany: Geophysics, **77**, KS13–KS31.

Hamdi, F.A.I., and Smith, D.T., 1981, Soil consolidation behavior assessed by seismic velocity measurement: Geophys. Prosp., **29**, 715–729.

Hanafy, Sh.M., 2005, Seismic refraction interpretation using finite difference method: *in* Proceedings: Symposium on the Applications of Geophysics to Engineering and Environmental Problems, 1012–1024.

Hanafy, Sh.M., 2010, Locating of sinkhole extension by seismic refraction tomography and GPR methods: *in* Expanded Abstracts: 72nd EAGE Conference and Exhibition, doi:10.3997/2214-4609.201401144.

Hanafy, Sh.M., 2012, Subsurface fault and colluvial wedge detection using resistivity, refraction tomography and seismic reflection: *in* Expanded Abstracts: 74th EAGE Conference and Exhibition, doi:10.3997/2214-4609. 20148516.

Hanafy, Sh.M., and Schuster, G.T., 2011, Two applications of time reversal mirrors: Seismic radio and seismic radar: J. Acoust. Soc. Am., **130**(3) 1985–1994, doi:10.1121/ 1.3621469.

Hanafy, Sh.M., Cao, W., McCarter, M., and Schuster, G.T., 2009, Using super-stacking and super-resolution properties of time reversal mirrors to locate trapped miners: The Leading Edge, **28**(3) 302–307.

Hawkins, L.V., 1961, The reciprocal method of routine shallow seismic refraction investigation: Geophysics, **26**, 806–819.

Hearne, T.M., Stokoe, K.H., and Reese, L.C., 1979, Drilled-shaft integrity by wave propagation method, *in* Geophys. Meth. in Geotech. Eng., preprint 3794, Am. Soc. Civil Eng.

Henriet, J.P., Schitrtekat, J., and Heidens, Ph. 1983, Borehole seismic profiles and tube wave applications in a dam site investigation: Geophys. Prosp., **31**, 72–86.

Holzhausen, G.R., Card, C.C., Raisbeck, J.M., and Dobecki, T.L., 1985, Hydraulic fracture growth during steam stimulation in a single-well test: 55th Ann. Ca1if. Reg. Mtg. of Soc. Petr. Eng. Am. Inst. Min. Metall. Petr. Eng., Paper SPE 13619.

Imai, T., Fumoto, H., and Yokota, K., 1976, P- and S-wave velocities in subsurface layers of ground in Japan: Urawa Research Institute, Tokyo, 2384 pp.

International Atomic Energy Agency, 1972, Earthquake guidelines for reactor siting: Tech. Rep. Series, No. 139, Vienna.

Khalil, M.H., and Hanafy, Sh.M., 2008, Engineering applications of geophysics: A field example at Wadi Wardan, northeast Gulf of Suez, Sinai, Egypt: Journal of Applied Geophysics, **65**(3-4) 132–141, doi:10.1016/j.jappgeo. 2008.06.003.

Kim, J.T., Kim, D.S., Park, H.J., Bang, E.S., and Kim, S.W., 2010, Evaluation of the applicability of the surface wave method to rock fill dams: Exploration Geophysics, **41**(1) 9–23.

Moayed, R.Z., 2012, Effect of elastic modulus varieties in depth on subgrade reaction modulus of granular soils: Second International Conference on Geotechnique, Construction Materials and Environment, Kuala Lumpur, Malaysia, ISBN: 978-4-9905958-1-4 C3051.

Nolan, J., Sloan, S.D., Broadfoot, S.W., McKenna, R., and Metheny, O.M., 2011, Nearsurface void identification using MASW and refraction tomography techniques: *in* Expanded Abstracts: 81st International Annual Meeting, Society of Exploration Geophysicists, **30**, 1401–1405.

Parry, R.H., 1977, Estimating bearing capacity of sand from SPT values: JGED, ASCE, **103**, 1014–1043.

Qin, F., Luo, Y., Olsen, K.B., Cai, W., and Schuster, G.T., 1992, Finite-difference solution of the eikonal equation along expanding wavefronts: Geophysics, **57**, 478–487.

Said, R., 1962, The geology of Egypt: Elsevier Pub. Co., Amsterdam and New York, 337 pp.

Said, R., 1990, The geology of Egypt: Balkema, Rutterdam.

Shan, G., Bastani, M., Malehmir, A., Persson, L., and Engdahl, M., 2014, Integrated 2D modeling and interpretation of geophysical and geotechnical data to delineate quick clays at a landslide site in southwest Sweden: Geophysics, **79**(4) EN61–EN75.

Sheriff, R.E., 2002, Encyclopedic dictionary of applied geophysics 4th ed.: Society of Exploration Geophysicists, Tulsa, Oklahoma, 163 pp.

Sheriff, R.E., and Geldart, L.P., 1986, Exploration seismology: Cambridge Univ. Press, Cambridge, 316 pp.

Sjogren, B., Ofsthus, A., and Sandberg, J., 1979, Seismic classification of rock mass qualities: Geophys. Prosp., **27**, 409–442.

Sobreira, J.F.F., Lipski, M., Carvalho, L., and Marquez, E., 2010, Geotechnical characterization based on seismic data approaches applied on Campos basin, southeastern Brazilian margin: The Leading Edge, **29**(7) 842–846.

Stumpel, H., Kahler, S., Meissner, R., and Milkereit, B., 1984, The use of seismic shear waves and compressional waves for lithological problems of shallow sediment: Geophys. Prosp., **32**, 662–675.

Tatham, R.H., 1982, Vp/Vs and lithology: Geophysics, **47**(3) 336–344.

Terzaghi, K., 1955, Evaluation of coefficient of subgrade reaction: Geotechnique, **5**, 297–326.

Tribedi, A., 2013, Correlation between soil bearing capacity and modulus of subgrade reaction: Structural Design, 16–20, http://www.structuremag.org/?p=1239.

U.S. Government, 1974, Code of Federal Regulations, 10 (10 CFR): Office of the Federal Register, U.S.G.P.O., Washington, D.C.

van Overmeeren, R.A., 1975, A combination of gravity and seismic refraction measurements applied to groundwater explorations near Taltal, Province of Antofagasta, Chile: Geophys. Prosp., **23**, 248–258.

van Overmeeren, R.A., 1980, Tracing by gravity of a narrow graben structure, detected by seismic refraction, for groundwater investigations in north Chile: Geophys. Prosp., **28**, 392–397.

van Overmeeren, R.A., 1981, A combination of electrical resistivity, seismic refraction, and gravity rneasurements for groundwater exploration in Sudan: Geophysics, **46**, 1304–1313.

Vandenberghe, I., 1976, Combined refraction seismic and gravimetric investigation in a paleogeographic and geologic research program: Geophys. Prosp., **24**, 371–379.

Vidale, J., 1988, Finite-difference calculation of traveltimes: Bull. Seismol. Soc. Am., **78**, 2062–2076.

Vidale, J., 1990, Finite-difference calculation of traveltimes in three dimensions: Geophysics, **55**, 521–526.

Worthington, P.F., 1976, Hydrogeophysical properties of parts of the British Trias: Geophys. Prosp., **24**, 672–695.

Worthington, P.F., 1977, Geophysical investigation of groundwater resources in the Kalahari Basin: Geophysics, **42**, 838–849.